

Disorders of the Nervous System

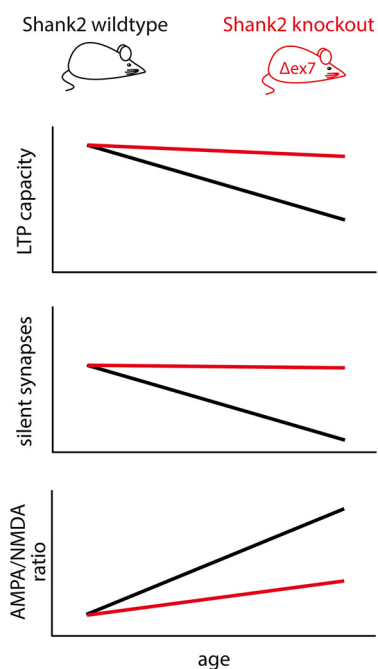
Defective Synapse Maturation and Enhanced Synaptic Plasticity in Shank2 $\Delta\text{ex}7^{-/-}$ Mice

Stephanie Wegener,¹ Arne Buschler,² A. Vanessa Stempel,¹ Sukjae J. Kang,³ Chae-Seok Lim,³ Bong-Kiun Kaang,³ Sarah A. Shoichet,⁴ Denise Manahan-Vaughan,² and Dietmar Schmitz⁵

DOI: <http://dx.doi.org/10.1523/ENEURO.0398-17.2018>

¹Neuroscience Research Center, Charité Universitätsmedizin, 10117 Berlin, Germany, ²Medical Faculty, Department of Neurophysiology, Ruhr University Bochum, 44801 Bochum, Germany, ³School of Biological Sciences, Seoul National University, Seoul 08826, Korea, ⁴Institute of Biochemistry and Cluster of Excellence NeuroCure, Charité Universitätsmedizin, 10117 Berlin, Germany, and ⁵Neuroscience Research Center, Cluster of Excellence NeuroCure, German Center for Neurodegenerative Diseases, Charité Universitätsmedizin, 10117 Berlin, Germany

Visual Abstract



Autism spectrum disorders (ASDs) are neurodevelopmental disorders with a strong genetic etiology. Since mutations in human *SHANK* genes have been found in patients with autism, genetic mouse models are used for a mechanistic understanding of ASDs and the development of therapeutic strategies. SHANKs are scaffold proteins in the postsynaptic density of mammalian excitatory synapses with proposed functions in synaptogenesis, regulation of dendritic spine morphology, and instruction of structural synaptic plasticity. In contrast to all studies so far on the function of SHANK proteins, we have previously observed enhanced synaptic plasticity in Shank2 $\Delta\text{ex}7^{-/-}$ mice. In a series of experiments, we now reproduce these results, further explore the synaptic phenotype, and directly compare our model to the independently generated Shank2 $\Delta\text{ex}6-7^{-/-}$ mice. Minimal stimulation experiments reveal that Shank2 $\Delta\text{ex}7^{-/-}$ mice possess an excessive fraction of silent (i.e., α -amino-3-hydroxy-5-methyl-4-isoxazolepropionic acid, short, AMPA receptor lacking) synapses. The synaptic maturation deficit emerges during the third postnatal week and constitutes a plausible mechanistic explanation for the mutants' increased capacity for long-term potentiation, both *in vivo* and *in vitro*. A direct comparison with Shank2 $\Delta\text{ex}6-7^{-/-}$ mice adds weight to the hypothesis that both mouse models show a different set of synaptic phenotypes, possibly due to differences in their genetic background. These findings add to the diversity of synaptic phenotypes in neurodevelopmental disorders and further support the supposed existence of "modifier genes" in the expression and inheritance of ASDs.

Key words: autism; LTP; maturation; PSD; shank; synapse

Significance Statement

Autism spectrum disorders have a global prevalence of 0.1–2%, a fraction of which is caused by mutations in human *SHANK* genes. A number of Shank mouse models that reproduce behavioral symptoms also show reduced synaptic plasticity, which is why boosting plasticity has become one line of therapeutic rescue efforts. In contrast to all studies so far on the function of SHANK proteins, we observe enhanced plasticity in Shank2 $\Delta\text{ex}7^{-/-}$ mice and uncover a previously unrecognized synapse maturation deficit. This neurodevelopmental phenotype is shared among a number of mouse models for neurodevelopmental disorders, suggesting synapse maturation as a field of future studies and for the exploration of therapeutic intervention. The observation of distinct and noncongruent phenotypes in genetically similar yet nonidentical mouse models adds weight to the hypothesis that genetic interactions of putative "modifier genes" might influence the phenotype.

Introduction

The activity-dependent formation and remodeling of synaptic connections is pivotal to adaptive neural circuit function. Dysregulation of these processes is considered a prime cause of neurodevelopmental diseases such as autism spectrum disorders (ASDs; Ebert and Greenberg, 2013). The list of mutations associated with ASDs and the number of mouse models is growing rapidly, yet understanding the connections among genetic mutation, synaptic defects, and disease phenotypes remains a challenge.

Mutations in all three *SHANK* genes (*SHANK1*, *SHANK2*, and *SHANK3*) occur in autistic patients (Durand et al., 2007; Berkel et al., 2010; Sato et al., 2012), and Shank mutant mice reproduce several autism-related phenotypes (Bozdagi et al., 2010; Peça et al., 2011; Wang et al., 2011; Schmeisser et al., 2012; Won et al., 2012; Lee et al., 2015; Peter et al., 2016). SHANKs (short for SH3 and multiple ankyrin repeat domains protein, also referred to as ProSAPs) are scaffold proteins in the postsynaptic density of mammalian excitatory synapses, linking postsynaptic membrane proteins to the cytoskeleton (for review, see Sheng and Kim, 2000) to serve functions in synaptogenesis (Du et al., 1998; Roussignol et al., 2005), regulation of dendritic spine morphology (Sala et al., 2001; Haeckel et al., 2008; Kim et al., 2009; Verpelli et al., 2011; Durand et al., 2012), and instruction of structural synaptic plasticity (MacGillavry et al., 2016).

Considerable efforts have been made to understand and differentiate the roles of different Shank isoforms in synaptic function and ASD pathophysiology (for review, see Jiang and Ehlers, 2013). The picture is complicated by diverging reports on the synaptic pathophysiology of mice lacking Shank2: for two independently generated Shank2 knock-out (KO) mice, noncongruent results on long-term plasticity and excitatory synaptic transmission were reported in two independent studies (Shank2 $\Delta\text{ex}7^{-/-}$, Schmeisser et al., 2012; Shank2 $\Delta\text{ex}6-7^{-/-}$, Won et al.,

2012), and differences in inhibitory synaptic transmission were found in a direct comparison of the two mouse models (Lim et al., 2017).

To consolidate and mechanistically advance our understanding of excitatory synaptic transmission in Shank2 knock-out mice, we here report robustly increased long-term potentiation (LTP) in Shank2 $\Delta\text{ex}7^{-/-}$ mice upon electric stimulation *in vitro* and also *in vivo*. We find that Shank2 $\Delta\text{ex}7^{-/-}$ mice suffer from deficient synaptic maturation and an increased fraction of AMPA receptor-lacking synapses, suggesting a mechanistic explanation for their increased LTP capacity. A direct comparison of *in vivo* LTP in Shank2 $\Delta\text{ex}6-7^{-/-}$ and Shank2 $\Delta\text{ex}7^{-/-}$ mice reveals further differences between the two mouse models, supporting the idea of genetic interactions in the Shank2 mouse model (Lim et al., 2017), paralleling observations of putative modifier genes in the expression and inheritance of ASDs (Leblond et al., 2012).

Materials and Methods

Shank2 $\Delta\text{ex}7$ (Schmeisser et al., 2012) and Shank2 $\Delta\text{ex}6-7$ mice (Won et al., 2012) were bred on a C57BL/6J background with a heterozygous breeding protocol. The study was conducted in accordance with the European Communities Council Directive of September 22, 2010 (2010/63/EU) for care of laboratory animals and after approval by the local ethics and/or animal welfare committees [Berlin animal experiment authorities and the Animal Welfare Committee of the Charité Berlin (File reference: T100/03), and Landesamt für Naturschutz, Verbraucherschutz und Umweltschutz, Nordrhein Westfalen, respectively]. Wild-type littermates were used as a control throughout, and experimenters were blind to the genotype of the tested animals for data collection and analysis.

Hippocampal brain slices were prepared from animals of both sexes as described previously (Schmeisser et al., 2012). Briefly, mice were anesthetized with isoflurane and decapitated. Brains were rapidly removed and transferred to ice-cold ACSF slicing solution. The ACSF slicing solution contained the following (in mM): 87 NaCl, 26 NaHCO₃, 50 sucrose, 25 glucose, 3 MgCl₂, 2.5 KCl, 1.25 NaH₂PO₄, and 0.5 CaCl₂. The ACSF recording solution contained the following (in mM): 119 NaCl, 26 NaHCO₃, 10 glucose, 2.5 KCl, 2.5 CaCl₂, 1.3 MgCl₂, and 1 NaH₂PO₄. All ACSF was equilibrated with carbogen (95% O₂, 5% CO₂). Tissue blocks containing the hippocampus were mounted on a Vibratome (VT1200, Leica) and cut into horizontal slices of 300 μm . For submerged slice storage (used for minimal stimulation experiments), slices were, after preparation, kept submerged in ACSF at 34°C for 30 min, then slowly cooled to room temperature where they were left to recover for at least 30 min up to 5 h. Recordings were performed in slices submerged in ACSF and at room temperature. For a subset of experiments (Fig. 1), we reproduced a range of conditions from the study by Won et al. (2012): immediately after preparation, slices were transferred into an ACSF/oxygenated air interface chamber and allowed to remain there to recover until recording, for at least 1 h and at most 5 h. Recordings were performed in a submerged recording chamber; the storage and re-

Received November 20, 2017; accepted May 7, 2018; First published May 29, 2018.

The authors declare no competing financial interests.

Author contributions: S.W., A.B., A.V.S., S.J.K., C.S.-L., B.K.-K., S.A.S., D.M.-V., and D.S. designed research; S.W., A.B., and A.V.S. performed research; S.W., A.B., and D.M.-V. analyzed data; S.W. wrote the paper.

This research was supported by NeuroCure (Grant Exc257), Bernstein Center for Computational Neuroscience, Einstein Foundation, and Deutsche Forschungsgemeinschaft (Grants SFB665, SFB874/B1, SFB958, SFB1280/A4, SPP1665, GRK1123, and SH650/2-1).

S. Wegener's present address: Janelia Research Campus, Howard Hughes Medical Institute, Ashburn VA 20147.

A.V. Stempel's present address: Sainsbury Wellcome Centre, UCL, London W1T 4JG, UK.

Acknowledgements: We thank Susanne Rieckmann, Anke Schönherr, and Karin Bloch for assistance with mouse breeding; Dr. Christa Thöne-Reineke for overseeing animal transports; and Stephan Jansen for technical assistance with the *in vivo* experiments.

Correspondence should be addressed to Stephanie Wegener, Janelia Research Campus, Howard Hughes Medical Institute, Ashburn VA 20147. E-mail: wegeners@janelia.hhmi.org.

DOI: <http://dx.doi.org/10.1523/ENEURO.0398-17.2018>

Copyright © 2018 Wegener et al.

This is an open-access article distributed under the terms of the Creative Commons Attribution 4.0 International license, which permits unrestricted use, distribution and reproduction in any medium provided that the original work is properly attributed.

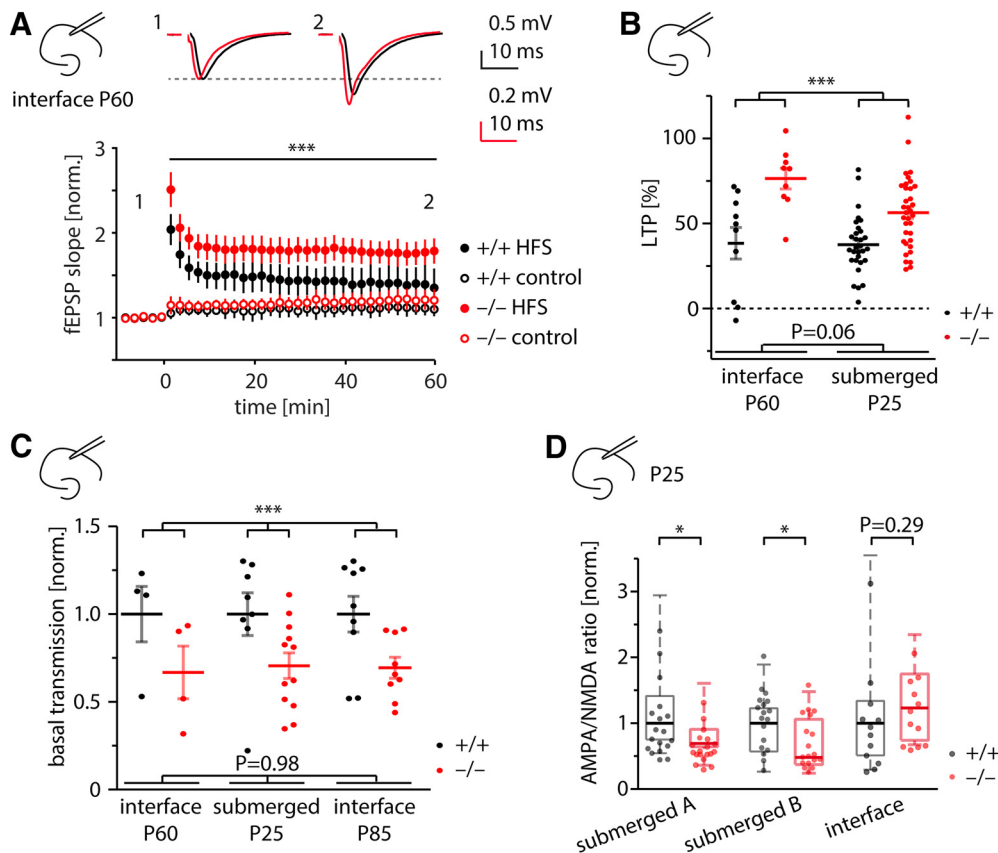


Figure 1. Enhanced LTP and reduced basal transmission in Shank2 $\Delta\text{ex}7^{-/-}$ mice *in vitro*. **A**, Enhanced LTP in Shank2 $\Delta\text{ex}7^{-/-}$ mice *in vitro*. NMDA receptor-dependent LTP in the CA1 region of corticohippocampal slices was induced by high-frequency stimulation protocol (HFS; closed symbols). In a subset of experiments (+/+, 5/10; -/-, 7/9), synaptic responses of a nonpotentiated fiber tract were recorded as an additional control (control; open symbols). Example traces at top. *** $p = 0.0025$ [difference between genotypes in a two-way ANOVA; $n(N)_{+/+} = 10(3)$, $n(N)_{-/-} = 9(3)$]. Slices were stored in an ACSF/oxygenated air interface chamber as reported by Won et al. (2012). **B**, Increased LTP in Shank2 $\Delta\text{ex}7^{-/-}$ mice is irrespective of animal age and slice storage. Submerged data replotted from Schmeisser et al. (2012). Significance was tested with two-way ANOVA *** $p < 0.0001$ for genotype comparison across conditions. **C**, Decreased basal synaptic transmission in Shank2 $\Delta\text{ex}7^{-/-}$ mice irrespective of animal age and slice storage. Basal transmission for each experiment is expressed as a single slope fitted to the input–output function of fEPSP slope vs fiber volley. Slopes of each group are normalized to the population mean of the wild type in the respective recording condition. Submerged data (P25) from the study by Schmeisser et al. (2012) are reanalyzed. Significance was tested with two-way ANOVA. *** $p = 0.0005$ for genotype comparison across conditions. **D**, Slice storage conditions affect AMPA/NMDA receptor ratios. Significance was tested with Mann–Whitney U test. AMPA/NMDA receptor ratios are significantly reduced in CA1 pyramidal cells of Shank2 $\Delta\text{ex}7^{-/-}$ mice when slices are stored submerged in ACSF before recording [submerged 1: $p = 0.013$ data replotted from the study by Schmeisser et al., 2012; submerged 2: $p = 0.036$; see also Fig. 4B], but not when stored in an ACSF/oxygenated air interface chamber. Mouse age was 3–4 weeks for all groups.

recording temperature for these experiments was 34°C. Mouse age for *in vitro* experiments was 8–9 weeks for the experiments shown in Figure 1A and 3–4 weeks for experiments in Figure 1D and Figure 4A–D. For the remaining *in vitro* experiments (Figs. 1B,C, 4E), mouse age is indicated in the figure legend.

For all *in vitro* experiments, data were recorded with an Axopatch 700A Amplifier (Molecular Devices), digitized at 5 kHz, filtered at 2 kHz, and recorded in IGOR Pro 4.0. Evoked postsynaptic responses were induced by stimulating Schaffer collaterals in CA1 stratum radiatum. Field EPSPs (fEPSPs) were recorded in stratum radiatum. fEPSP rising slopes were fitted to 20–80% of the fEPSP amplitude. LTP was induced by a single tetanus of 100 pulses at 100 Hz. For whole-cell patch-clamp recordings, the recording ACSF was supplemented with 1 μM gaba-

zine. Pipettes had resistances of 2–3 M Ω . Liquid junction potential was not corrected. Series resistance (not compensated) was constantly monitored and was not allowed to increase beyond 22 M Ω or change by >20% during the experiment. Compound EPSCs were recorded at –60 and +40 mV with a cesium-based intracellular recording solution containing the following (in mM): 145 CsCl, 10 HEPES, 0.2 EGTA, 2 MgCl₂, 2 NaATP, 0.5 NaGTP, and 5 phosphocreatine, with osmolarity of 305 mOsm and pH adjusted to 7.2 with CsOH. The AMPA receptor-mediated component of the EPSC was estimated by measuring the peak amplitude of the averaged EPSC at –60 mV. The N-methyl-D-aspartate, short, NMDA receptor-mediated component was estimated at +40 mV by measuring the amplitude of the averaged EPSC 25 ms after stimulation.

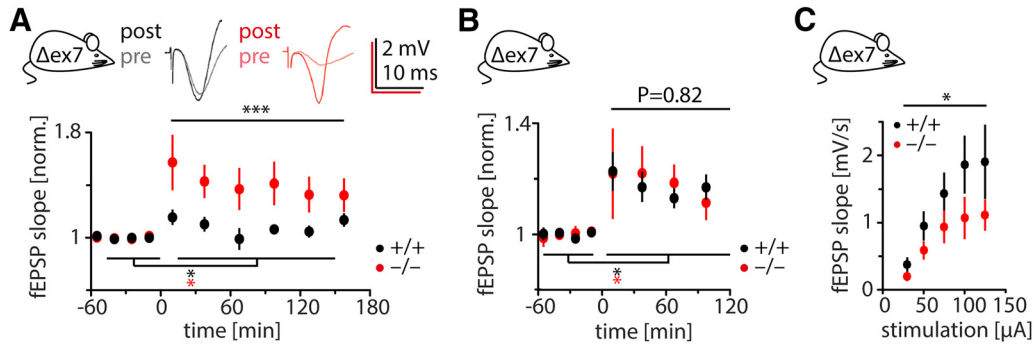


Figure 2. Enhanced LTP and reduced basal transmission in Shank2 $\Delta\text{ex}7^{-/-}$ mice *in vivo*. **A**, Enhanced LTP in Shank2 $\Delta\text{ex}7^{-/-}$ mice *in vivo*. 3h-LTP was induced at time point “0” by high-frequency stimulation in awake, freely behaving mice (for details, see Materials and Methods). Example traces are at top. LTP was induced in both genotypes (ANOVA; *: $+/+$, $p = 0.017$, $N = 16$; $-/-$: $p < 0.0001$, $N = 15$) but was significantly larger in Shank2 $\Delta\text{ex}7^{-/-}$ mice ($***p < 0.0001$, difference between genotypes in a two-way ANOVA). **B**, 2h-LTP was induced by mild high-frequency stimulation in awake, behaving mice (for details, see Materials and Methods). Significance was tested with two-way ANOVA. LTP was induced in both genotypes (*: $+/+$, $p < 0.0001$, $N = 16$; $-/-$, $p = 0.0019$, $N = 16$) with no significant difference between genotypes. **C**, Basal synaptic transmission in awake, behaving mice is reduced in Shank2 $\Delta\text{ex}7^{-/-}$ mice compared with wild-type controls. * $p = 0.011$ (difference between genotypes in a two-way ANOVA; $N_{+/+} = 12$; $N_{-/-} = 8$).

For minimal stimulation, the stimulation frequency was 0.2 Hz, and the stimulation electrode was placed to produce a single-peak response. At +40 mV holding potential, stimulation intensity was reduced until transmission failures were observed (in ~10–40% of events), and 20–50 events were recorded. Cells were subsequently clamped to –60 mV holding potential, and 30–50 events were recorded at the same stimulation intensity. In a subset of experiments, this order was reversed [i.e., stimulation intensity was adjusted and miniature EPSCs (minEPSCs) were recorded at –60 mV first, before cells were clamped to +40 mV]. We did not observe systematic differences in failure rates (r_f) or amplitudes of minEPSCs between the two regimes. Experiments with linearly increasing or decreasing failure rates and/or minEPSCs amplitudes at any holding potential were excluded from the analysis. *Post hoc* analysis counted a failure at depolarized potentials whenever the minEPSCs charge 5–40 ms after stimulation did not exceed a threshold of 0.9 pC. Failures at hyperpolarized potentials were defined as events with an minEPSCs peak smaller than twice the signal noise (i.e., the SD of the signal in a 3 ms time window averaged over all sweeps at a certain holding potential) of that recording. The average signal noise was not different among experimental groups, and experiments with high background noise were excluded from the analysis. While the absolute failure rates depended on how the criteria for failure versus successes were set, the relative difference between genotypes did not. For each experiment, the synaptic potency was defined as the average amplitude of all minEPSCs at a given holding potential that qualified as successes. For EPSCs recorded at –60 mV, the amplitude was taken at the peak of all individual EPSCs after subtraction of the average failure (for removal of the stimulus artifact). For EPSCs recorded at +40 mV, the amplitude was read 25 ms after stimulation. Synaptic transmission under minimal stimulation can be described by a Poisson distribution: $P(k) = (m^k e^{-m})/k!$ with $P(k)$ being the probability of k quanta being released and m being the

mean quantal content. Since the failure rate $r_f = P(0) = e^{-m}$, the fraction of silent synapses can be estimated as $1 - \ln(r_{f-60\text{mV}} - r_{f+40\text{mV}})$ (Liao et al., 1995) and the synaptic potency $S = -\ln(r_f) * q$, with q being the mean quantal size.

For *in vivo* experiments, 7- to 8-week-old male mice were implanted (under anesthesia) with a stimulation electrode in the Schaffer collaterals (2.0 mm posterior and 2.0 mm lateral to bregma) and a recording electrode in the stratum radiatum of the dorsal CA1 region (1.9 mm posterior and 1.4 mm lateral to bregma), as described previously (Buschler et al., 2012). Animals recovered for ~10 d before experiments were commenced. Before each experiment, input/output (I/O) properties were recorded by increasing the stimulation intensity stepwise (Fig. 2C). Experiments were conducted in recording chambers [20 (length) × 20 (width) × 30 (height) cm] where animals could move freely and had access to food and water *ad libitum*. During recordings, implanted electrodes were connected via a flexible cable and a rotatable commutator to the stimulation unit and amplifier. Test-pulse stimulation was set to elicit 40% of the maximal I/O response. Stimuli of 0.2 ms duration were applied at a frequency of 0.025 Hz and recorded with a sample rate of 10 kHz. Different protocols were used to elicit LTPs of differing magnitudes and durations (Buschler et al., 2012), all NMDA receptor dependent (Ballesteros et al., 2016). Two induction protocols were found to elicit robust LTP that was stable for >3 h (3h-LTP). Protocol 1 contained four trains of 50 pulses at 100 Hz with a 5 min intertrain interval (Shank2 $\Delta\text{ex}7$: $N_{+/+} = N_{-/-} = 8$; Shank2 $\Delta\text{ex}6-7$: $N_{+/+} = N_{-/-} = 5$). Protocol 2 contained 2 trains of 50 pulses at 200 Hz with 5 min intertrain interval (Shank2 $\Delta\text{ex}7$: $N_{+/+} = 8$, $N_{-/-} = 7$; Shank2 $\Delta\text{ex}6-7$: $N_{+/+} = N_{-/-} = 5$). Results from both protocols were quantitatively similar and pooled for Figures 2A and 3A, respectively. Two protocols elicited LTP that was short lived, receding back to baseline in ~2 h (2h-LTP): protocol 3, a single train of 50 pulses at 100 Hz stimulation (Shank2 $\Delta\text{ex}7$: $N_{+/+} = N_{-/-} =$

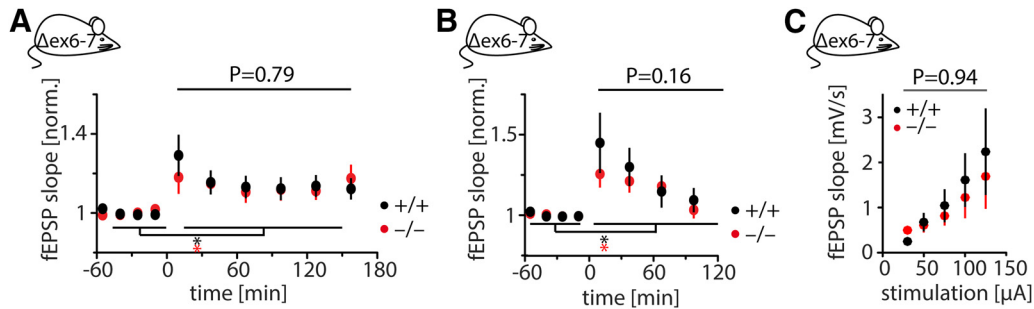


Figure 3. *In vivo* LTP in Shank2 $\Delta\text{ex6-7}^{-/-}$ mice. **A**, High-frequency stimulation at time point “0” successfully induced 3h-LTP in Shank2 $\Delta\text{ex6-7}^{-/-}$ and wild-type mice (*: +/+, $p < 0.0001$, $N = 10$; -/-, $p = 0.012$, $N = 10$) with no detectable difference between genotypes. Significance was tested by two-way ANOVA. **B**, 2h-LTP was successfully induced in both genotypes (*: +/+, $p < 0.0001$, $N = 10$; -/-, $p < 0.001$, $N = 10$). A trend for reduced potentiation in Shank2 $\Delta\text{ex6-7}^{-/-}$ mice did not reach significance ($p = 0.16$, difference between genotypes in a two-way ANOVA). **C**, Basal synaptic transmission in awake, behaving mice is not significantly different in Shank2 $\Delta\text{ex6-7}^{-/-}$ mice compared with wild-type controls ($p = 0.94$, difference between genotypes in a two-way ANOVA; $N_{+/+} = N_{-/-} = 5$).

8; Shank2 $\Delta\text{ex6-7}$: $N_{+/+} = N_{-/-} = 5$); and protocol 4, two trains of 50 pulses at 100 Hz stimulation with a 5 min intertrain interval (Shank2 Δex7 : $N_{+/+} = N_{-/-} = 8$; Shank2 $\Delta\text{ex6-7}$: $N_{+/+} = N_{-/-} = 5$). Results from protocols 3 and 4 were quantitatively similar and pooled for Figures 2B and 3B, respectively. Statistical tests for the expression of LTP within an experimental group involved comparing post-tetanus responses to pretetanus baseline responses with time as a continuous variable (with all time points before induction set to 0 min) and preinduction/postinduction as a categorical variable. Tests between genotypes compared postinduction time points only, with time as a continuous variable and genotype as a categorical variable. Potentiation in text and Table 1 was quantified at 2–3 h postinduction for 3h-LTP and 1–2 h postinduction for 2h-LTP.

Analyses were performed using custom-written procedures in IGOR Pro and MATLAB. Data in graphs and text are, unless stated otherwise, presented as the mean \pm SE for parametric data and the median [25th 75th percentile] for nonparametric data (graphically, whiskers additionally represent the minimum and maximum values). Unpaired two-tailed Student’s t test (short: Student’s t test) and ANOVAs were used to test for the statistical significance of parametric data, and Mann–Whitney U tests and Kruskal–Wallis tests were used for nonparametric data. Results were considered to be significant at $p < 0.05$. Curve fitting was performed in MATLAB using a nonlinear least-squares algorithm. Stimulus artifacts were blanked or cropped in sample traces. Sample sizes are given as the number of experiments and the number of animals (N).

Results

Two parallel studies on genetically similar Shank2 $^{-/-}$ mice have reported increased LTP (Schmeisser et al., 2012) and decreased LTP (Won et al., 2012), respectively, in hippocampal brain slices of Shank2-null mutants. To investigate whether biological or methodological differences account for this discrepancy, we first investigated in Shank2 $\Delta\text{ex7}^{-/-}$ mice (Schmeisser et al., 2012) how differences in slice storage, recording temperature, and animal age might affect the expression of LTP. To this

end, we reproduced a range of conditions from the study by Won et al. [2012]; i.e., slices were stored in an ACSF/oxygenated air (Haas type) interface chamber instead of submerged in ACSF before recording; animal age was 8–9 weeks instead of 3–4 weeks, and recordings were performed at elevated temperature instead of room temperature]. Hippocampal slices from Shank2 $\Delta\text{ex7}^{-/-}$ mice were then subjected to the common LTP induction protocol (for details, see Materials and Methods). In our hands, also in these conditions, Shank2 $\Delta\text{ex7}^{-/-}$ mice showed markedly higher LTP than wild-type controls [WT, $38 \pm 9\%$; KO, $76 \pm 6\%$; $N_{+/+} = 10(3)$; $N_{-/-} = 9(3)$; Fig. 1A].

Since the studies on Shank2 $\Delta\text{ex7}^{-/-}$ and Shank2 $\Delta\text{ex6-7}^{-/-}$ mice also reported different phenotypes with respect to excitatory basal synaptic transmission and synaptic AMPA/NMDA ratios, we assessed these physiologic parameters as well. A quantitative comparison between results from the previous study (Schmeisser et al., 2012) and new experiments is presented in Figure 1B–D. Slice storage affected phenotypes to varying degrees: While in our hands storing slices submerged in ACSF versus a Haas-type interface chamber before recording had no effect on the expression of LTP ($p = 0.89$ for comparison of experimental conditions in a two-way ANOVA; Fig. 1B) or basal synaptic transmission ($p = 0.98$ for comparison of experimental conditions in a two-way ANOVA; Fig. 1C), it did affect AMPA/NMDA receptor ratios (Fig. 1D), with a trend toward an increased AMPA/NMDA ratio in slices of Shank2 $\Delta\text{ex7}^{-/-}$ mice that have been stored in an interface chamber (Mann–Whitney U test, $p = 0.29$) compared with significantly reduced AMPA/NMDA ratio in slices that have been stored in submerged conditions (Mann–Whitney U test, $p = 0.013$ and $p = 0.036$ for two independent datasets; Fig. 1D). Increased AMPA/NMDA ratios have been reported in Shank2 $\Delta\text{ex6-7}^{-/-}$ mice (Won et al., 2012); we thus conclude that the experimental conditions examined here might explain some diverging results in Shank2 $\Delta\text{ex7}^{-/-}$ versus Shank2 $\Delta\text{ex6-7}^{-/-}$ mice, like AMPA/NMDA ratios, but not the contrary observations on basal synaptic transmission and LTP.

Table 1. Details of statistical analyses presented in the article

Figures	Experiment	n(N)	Test used	p value	Mean (CI)*
1A	<i>In vitro</i> , interface, P55	WT: 10(3), KO: 9(3)	ANOVA	0.0025	see 1B _{left}
1B	Left: <i>in vitro</i> , interface, P55	WT: 10(3), KO: 9(3)	Two-way ANOVA	Experimental condition: 0.89 genotype: <0.0001	WT: 38.3 (18.2), KO: 76.4 (12.0)
	Right: <i>in vitro</i> , submerged, P25	WT: 30(5), KO: 34(6)			WT: 37.6 (6.1), KO: 56.3 (6.9)
1C	Left: <i>in vitro</i> , interface, P25	WT: 4(2), KO: 4(2)	Two-way ANOVA	Experimental condition: 0.98 genotype: 0.0005	WT: 1.00 (0.31), KO: 0.67 (0.29)
	Middle: <i>in vitro</i> , submerged, P25	WT: 8(3), KO: 11(4)			WT: 1.00 (0.24), KO: 0.71 (0.14)
	Right: <i>in vitro</i> , interface, P85	WT: 9(3), KO: 9(3)			WT: 1.00 (0.20), KO: 0.69 (0.12)
1D*	Left: <i>in vitro</i> , submerged, P25	WT: 18(8), KO: 19(6)	Mann-Whitney U	0.013	WT: 1.0 [0.8 1.4], KO: 0.7 [0.6 0.9]
	Middle: <i>in vitro</i> , submerged, P25	WT: 20(6), KO: 18(8)	Mann-Whitney U	0.036	WT: 1.0 [0.6 1.2], KO: 0.5 [0.4 1.1]
	Right: <i>in vitro</i> , interface, P25	WT: 12(2), KO: 12(2)	Mann-Whitney U	0.29	WT: 1.0 [0.5 1.3], KO: 1.2 [0.7 1.7]
2A	<i>In vivo</i> , P50, 3h-LTP	WT: 16, KO: 15	For LTP induction: two-way ANOVA	LTP (categorical): WT: 0.017, KO: <0.0001 time (continuous): WT: 0.42, KO: 0.005 genotype: <0.0001 time: 0.016	LTP 2-3h postinduction (%): WT: 9.1 (8.6), KO: 32.6 (25.5)
2B	<i>In vivo</i> , P50, 2h-LTP	WT: 16, KO: 16	For LTP induction: two-way ANOVA	LTP (categorical): WT: <0.0001, KO: 0.002 time (continuous): WT: 0.02, KO: 0.15 Genotype: 0.82 time: 0.048	LTP 1-2h postinduction (%): WT: 15.0 (6.9), KO: 15.0 (12.1)
2C	<i>In vivo</i> , P50	WT: 12, KO: 8	Two-way ANOVA	Genotype: 0.011 stimulation: <0.0001	WT _{125μA} : 1.9 (1.1), KO _{125μA} : 1.1 (0.5)
3A	<i>In vivo</i> , P50, L-LTP	WT: 10, KO: 10	For LTP induction: two-way ANOVA	LTP (categorical): WT: <0.0001, KO: 0.012 time (continuous): WT: 0.007, KO: 0.74 Genotype: 0.79 time: 0.17	LTP 2-3h postinduction (%): WT: 12.9 (11.2), KO: 14.3 (12.0)
3B	<i>In vivo</i> , P50, E-LTP	WT: 10, KO: 10	For LTP induction: two-way ANOVA	LTP (categorical): WT: 0.0002, KO: <0.0001 time (continuous): WT: 0.022, KO: 0.003 Genotype: 0.16 time: 0.006	LTP 1-2h postinduction (%): WT: 12.0 (18.6), KO: 10.6 (13.2)
3C	<i>In vivo</i> , P50	WT: 5, KO: 5	Two-way ANOVA	Genotype: 0.94 stimulation: <0.0001	WT _{125μA} : 2.2 (1.9), KO _{125μA} : 1.7 (1.4)
4A	<i>In vitro</i> , submerged, P25	WT: 11(6) KO: 14(6)	Student's t test (paired)	WT: 0.19 KO: 0.0003	WT _{-60mV} : 16.3 (6.6), WT _{+40mV} : 13.2 (5.6) KO _{-60mV} : 36.3 (10.9), KO _{+40mV} : 12.7 (4.1)
4C	<i>In vitro</i> , submerged, P25	WT: 11(6), KO: 13(6)	Student's t test	0.0018	WT: 3.1 (4.4), KO: 23.6 (9.4)
4D*	<i>In vitro</i> , submerged, P25	WT: 20(6), KO: 18(8)	Mann-Whitney U	0.036	WT: 1.9 [1.1 2.3], KO: 0.9 [0.7 2.0]
4E	<i>In vitro</i> , submerged, AMPA/NMDA ratio*	P13-P14: WT: 16(4) KO: 18(5) P21-P24: WT: 10(3), KO: 11(3) P25-P28: WT: 10(4), KO: 7(3)	Over age groups: Kruskal-Wallis test Between genotypes: Mann-Whitney U	WT: 0.0026, KO: 0.056 P13-P14: 0.055 P21-P24: 0.083 P25-P28: 0.016	P13-P14: WT: 0.68 [0.47 0.88], KO: 0.45 [0.31 0.64] P21-P24: WT: 0.75 [0.55 1.09], KO: 0.63 [0.43 0.93] P25-P28: WT: 1.20 [0.88 1.48], KO: 0.78 [0.50 1.00]
	<i>In vitro</i> , submerged, LTP	P13-P14: WT: 10(2), KO: 7(2) P21-P24: WT: 15(2), KO: 14(2) P25-P28: WT: 15(3), KO: 20(3)	Over age groups: ANOVA Between genotypes: Student's t test	WT: 0.012, KO: 0.77 P13-P14: 0.30 P21-P24: 0.09 P25-P28: 0.0002	P13-P14: WT: 51.6 (12.9), KO: 61.6 (11.4) P21-P24: WT: 44.6 (7.9), KO: 58.2 (13.2) P25-P28: WT: 30.5 (8.2), KO: 55.3 (7.8)

* Median and percentiles [25th 75th] are reported for nonparametric datasets instead of mean and CI values.

In light of these results and reports on substantial changes in synaptic spine morphology after brain slice preparation (Kirov et al., 1999), we reasoned that an *in vitro* examination of Shank2^{-/-} phenotypes might be problematic, given that SHANK2 has a well described role in synaptogenesis and the regulation of structural dynamics in dendritic spines (MacGillavry et al., 2016). More precisely, we still wondered whether the decreased basal synaptic transmission and increased LTP we consistently observed in Shank2 Δex7^{-/-} mice might be secondary to slicing-induced synaptic remodeling. This motivated us to examine synaptic transmission and NMDA receptor-dependent LTP *in vivo*. Using established experimental

procedures (Buschler et al., 2012; for details, see Materials and Methods), we compared Shank2 Δex7^{-/-} and wild-type mice with regard to their capacity to express LTP *in vivo*. We tested different induction protocols, eliciting both short- and long-lasting forms of LTP in freely behaving mice (Buschler et al., 2012), from here on referred to as 2h-LTP and 3h-LTP, respectively (for details, see Materials and Methods). Both forms of LTP could be elicited in Shank2 Δex7^{-/-} mice and wild-type controls (Fig. 2A,B), validating that synapses without SHANK2 can express LTP, as our data from acute slices suggest. For 3h-LTP, the potentiation in Shank2 Δex7^{-/-} mice significantly exceeded that of wild-type controls [WT, 9 ± 4%

($N = 15$); KO, $33 \pm 13\%$ ($N = 16$); $p < 0.0001$ in a two-way ANOVA; Fig. 2A]. Further corroborating our *in vitro* results, basal synaptic transmission was significantly decreased in Shank2 $\Delta\text{ex}7^{-/-}$ mice versus wild-type controls when assessed in awake, behaving animals (Fig. 2C). In summary, we observe enhanced LTP and reduced synaptic basal transmission in Shank2 $\Delta\text{ex}7^{-/-}$ mice under a range of different conditions both *in vitro* and *in vivo*.

In contrast to Shank2 $\Delta\text{ex}7^{-/-}$ mice, Shank2 $\Delta\text{ex}6-7^{-/-}$ mice have been reported to show decreased LTP *in vitro* (Won et al., 2012; Peter et al., 2016), and genetic differences between the two mouse models have been suggested to account for this discrepancy (Lim et al., 2017). However, a direct comparison of excitatory synaptic transmission in the two models has so far been lacking. Thus, we next investigated *in vivo* LTP in freely behaving Shank2 $\Delta\text{ex}6-7^{-/-}$ mice. Both short- and long-lasting forms of LTP could be induced in wild-type as well as knock-out mice, with no significant difference in the magnitude of LTP expression (Fig. 3). A trend toward reduced short-lasting LTP in Shank2 $\Delta\text{ex}6-7^{-/-}$ mice was not stable over time (2h-LTP: WT, $12 \pm 10\%$ ($N = 10$); KO, $11 \pm 7\%$ ($N = 10$); $p = 0.16$ in a two-way ANOVA; Fig. 3B), although it was reminiscent of *in vitro* observations made by other laboratories (Won et al., 2012; Peter et al., 2016).

How can we understand the phenomena of reduced synaptic transmission and increased LTP in Shank2 $\Delta\text{ex}7^{-/-}$ mice? Is there a mechanistic explanation linking these two findings? In Shank3 $^{-/-}$ mice, reduced LTP has been associated with NMDA as well as AMPA receptor hypofunction (Wang et al., 2011; Kouser et al., 2013). Both mechanisms seem possible, since hippocampal CA1 LTP is dependent on both NMDA and AMPA receptors in its induction and expression, respectively (Nicoll, 2017). Shank2 $\Delta\text{ex}7^{-/-}$ mice show reduced AMPA receptor-dependent basal synaptic transmission (Fig. 1C), and, in submerged stored slices, a reduction in AMPA/NMDA ratios (Fig. 1D). In *Drosophila melanogaster*, animals lacking all SHANK isoforms show synaptic maturation deficits at the glutamatergic neuromuscular junction (Harris et al., 2016). We thus set out to test whether synapses lacking SHANK2 might possess fewer AMPA receptors or be functionally silent by lacking them altogether, rendering these synapses salient LTP substrates. To estimate the fraction of silent synapses, we performed minimal stimulation experiments. For each set of stimulated synapses, we recorded EPSCs at a holding potential of -60 mV (conducted by AMPA receptor-containing synapses) and at $+40$ mV, when synapses lacking AMPA receptors but harboring NMDA receptors can also pass currents. Indeed, minimal stimulation revealed markedly higher failure rates (r_f) in Shank2 $\Delta\text{ex}7^{-/-}$ mice than in wild-type controls at -60 mV but not at $+40$ mV [$r_{f,-60\text{mV}}$: WT, $16 \pm 3\%$; KO, $36 \pm 6\%$; $r_{f,+40\text{mV}}$: WT, $13 \pm 3\%$; KO, $13 \pm 2\%$; $N_{+/+} = 11(6)$, $N_{-/-} = 14(6)$; Fig. 4A], corresponding to a fraction of $\sim 51\%$ silent synapses in knock-out mice, compared with $\sim 11\%$ in wild-type controls. We next compared the transmission strength of individual synapses between Shank2 $\Delta\text{ex}7^{-/-}$ mice and wild-type mice. To that end, we expressed the apparent synaptic potency

S (the average amplitude of successfully evoked EPSCs) as a function of the observed failure rate r_f (which relates to the number of potentially active synapses) and fitted the mean quantal size q with $p = -\ln(r_f) * q$ (for details, see Materials and Methods). The average synaptic response estimated from this relationship was not different between Shank2 $\Delta\text{ex}7^{-/-}$ and wild-type mice for either NMDA receptor-mediated or AMPA receptor-mediated events (mean \pm CI; q_{NMDA} : WT, 4.4 ± 0.4 pA; KO, 4.3 ± 0.5 pA; q_{AMPA} : WT, -9.7 ± 2.7 pA; KO, -8.8 ± 3.1 pA; Fig. 4B). This suggests that it is mainly the higher difference in failure rates in Shank2 $\Delta\text{ex}7^{-/-}$ mice (Fig. 4C), and thus an excess of silent synapses, that accounts for the reduced AMPA/NMDA receptor ratio of the knockout (Fig. 4D).

It is conceivable that the increased fraction of silent synapses in Shank2 $\Delta\text{ex}7^{-/-}$ mice provides the structural framework for the increased LTP. To investigate how the two phenomena are correlated through maturation of the hippocampal circuitry, we repeated minimal stimulation and LTP experiments in juvenile mice [postnatal day 13 (P13) to P14]. At that age, wild-type and Shank2 $\Delta\text{ex}7^{-/-}$ mice alike showed high failure rates at hyperpolarized holding potentials and, consequently, a high fraction of silent synapses [silent synapses: WT, $\sim 48\%$; KO, $\sim 52\%$; r_f at -60 mV: WT, $43 \pm 6\%$; KO, $42 \pm 6\%$; r_f at $+40$ mV: WT, $19 \pm 2\%$; KO, $17 \pm 2\%$; $N_{+/+} = 16(7)$, $N_{-/-} = 18(7)$; t test over difference in failure rates between genotypes, $p = 0.76$]. Within the same age range, the magnitude of LTP evoked through tetanic stimulation was comparably high in both genotypes [WT, $52 \pm 7\%$; KO, $62 \pm 6\%$; $N_{+/+} = 10(2)$; $N_{-/-} = 7(2)$; $p = 0.3$, Student's t test], and AMPA/NMDA ratios were comparably low [WT, 0.71 ± 0.08 ; KO, 0.55 ± 0.08 ; $N_{+/+} = 16(7)$; $N_{-/-} = 18(7)$; $p = 0.055$, Mann-Whitney U test]. From P13 to P28, we saw significant synaptic maturation in juvenile wild-type mice (LTP, $p = 0.01$, ANOVA; AMPA/NMDA ratios, $p = 0.003$, Kruskal-Wallis) that was virtually absent in Shank2 $\Delta\text{ex}7^{-/-}$ mice (LTP, $p = 0.77$, ANOVA; AMPA/NMDA ratios, $p = 0.06$, Kruskal-Wallis test; Fig. 4E). We thus propose the deficient maturation of excitatory synapses in Shank2 $\Delta\text{ex}7^{-/-}$ mice as a possible cause for their decreased synaptic basal transmission, their decreased AMPA/NMDA ratios, and their increased capacity for LTP.

Discussion

In summary, we consistently observe increased LTP in hippocampal Schaffer collateral-CA1 synapses of Shank2 $\Delta\text{ex}7^{-/-}$ mice *in vitro* as well as in awake behaving animals. We have further uncovered a developmental synapse phenotype, an excess of silent synapses, that could link the phenomena of decreased synaptic transmission and increased LTP. During LTP expression, synaptic strength increases with the incorporation of AMPA receptors, a process through which immature, silent synapses (that previously lacked such receptors) can become unsilenced (Isaac et al., 1995; Liao et al., 1995; Durand et al., 1996). The idea that an increase in the number of silent synapses could provide a structural platform for the incorporation of additional AMPA receptors and hence a boost in LTP expression is corroborated by similar observations in

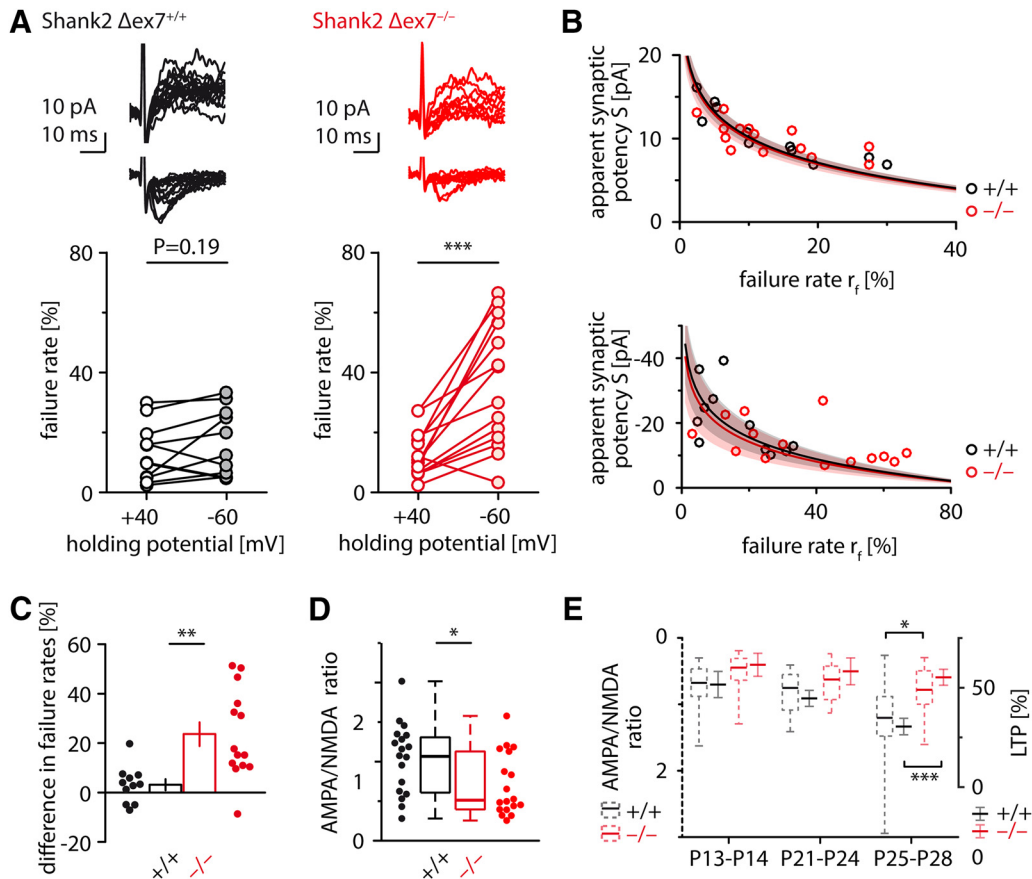


Figure 4. Minimal stimulation reveals insufficiently matured synapses in *Shank2 Δex7^{-/-}* mice. **A**, EPSCs were recorded at different holding potentials under minimal stimulation *in vitro*. Failure rates are plotted for control (left) and *Shank2 Δex7^{-/-}* mice (right). $***p = 0.0003$ [paired Student's *t* test. Example traces at top (top, EPSCs recorded at +40 mV; bottom, EPSCs recorded at -60 mV). **B**, For each holding potential, the apparent synaptic potency *S* (the average amplitude of all EPSCs) is expressed as a function of the failure rate r_f . Circles, line, and shaded area in black and red represent individual experiments, best fit, and the 95% confidence interval for wild-type and *Shank2 Δex7^{-/-}* mice, respectively (for details, see Materials and Methods). **C**, The respective difference between failure rates at hyperpolarized vs depolarized potentials ($r_{f -60mV} - r_{f +40mV}$) is significantly higher in *Shank2 Δex7^{-/-}* mice than in wild-type controls. $**p = 0.0018$ (Student's *t* test). **D**, AMPA/NMDA receptor ratios calculated from the average EPSC of minimal stimulation experiments are smaller in *Shank2 Δex7^{-/-}* mice than in wild-type controls (average is calculated across successes and failures alike). $*p = 0.036$ Mann-Whitney *U* test. **E**, Synaptic maturation in wild-type (black) and *Shank2 Δex7^{-/-}* mice (red) assessed in juvenile (P13–P14) and adolescent mice (P21–P28). Box plots (dashed) show AMPA/NMDA ratios from minimal stimulation experiments (left axis); mean and SE (nondashed) show LTP magnitude after tetanic stimulation (right axis). Significant differences can first be detected in mice aged P25–P28 (AMPA/NMDA ratios, $p = 0.016$, Mann-Whitney *U* test; LTP, $p = 0.0002$, Student's *t* test).

CamKIV^{-/-} mice acutely expressing constitutively active *CamKIV* variants (Marie et al., 2005) and observations in *PSD95^{-/-}* mice (Huang et al. 2015). A selective decrease in the number, but not the strength, of mature (AMPA receptor-containing) synapses is in good agreement with the results of a recent study on the effects of lentiviral-mediated SHANK2 knockdown in hippocampal slice culture (Shi et al., 2017) and relates to the reduction in frequency, but not amplitude, of spontaneously occurring mEPSCs in *Shank2 Δex7^{-/-}* mice (Schmeisser et al., 2012).

Why synaptic transmission is weak in *Shank2 Δex7^{-/-}* mice, although LTP can readily be induced *in vitro* and *in vivo*, remains to be elucidated. Similar observations have been made, however, upon acute knockdown of PSD-95 in hippocampal slice cultures (Ehrlich et al., 2007). It is conceivable that the loss of SHANK2 may be a reason for

decreased synaptic stability (Stanika et al., 2015) or the failure to instruct concomitant structural changes in potentiated synapses along with the early insertion of AMPA receptors (MacGillavry et al., 2016). Another open question is why, in our hands, AMPA/NMDA ratios in wild-type versus knockout animals are dependent on slice storage conditions. It is tempting to speculate that the hyperplasticity of synapses in *Shank2 Δex7^{-/-}* mice could influence their recovery after slice preparation.

At first sight, it seems peculiar that the *Shank2 Δex7^{-/-}* mouse line stands alone with its phenotype of increased LTP, while mouse lines with mutations in other *Shank* homologs show either no change in synaptic plasticity (*Shank1*, Hung et al., 2008) or reduced LTP (*Shank3*, Bozdagi et al., 2010; Kouser et al., 2013). However, considering the vast body of literature on isoform-specific

expression (Lim et al., 1999); protein–protein interactions (Lim et al., 2001; Boeckers et al., 2005); and spatiotemporal localization of SHANK1, SHANK2, and SHANK3 (Böckers et al., 2004; Grabrucker et al., 2011), different phenotypes in mutants lacking different isoforms are not surprising (Shi et al., 2017) and may in fact be indicators of isoform-specific functions of SHANK proteins in synapse formation, development, and plasticity.

Of note, Shank2 $\Delta\text{ex}6\text{--}7^{-/-}$ mice (Won et al., 2012) do not show increased *in vivo* LTP in our hands, in contrast to Shank2 $\Delta\text{ex}7^{-/-}$ mice. This difference between the two models is in line with earlier reports on their excitatory synaptic transmission (Schmeisser et al., 2012; Won et al., 2012) and parallels differences in their GABAergic physiology (Lim et al., 2017). When comparing these two Shank2 knockout mouse lines, isoform-specific differences in protein function fall short of explaining phenotypic differences, since both knockouts are null mutants on the SHANK protein level (Schmeisser et al., 2012; Won et al., 2012). The two mouse models exhibit differences in their genetic background, however, manifest in the differential expression of numerous genes (Lim et al., 2017). Resultant genetic interactions could be partly responsible for phenotypic variations and are in line with the supposed existence of “modifier genes” in the pathophysiology and etiology of ASDs (Leblond et al., 2012).

Shank2 $\Delta\text{ex}7^{-/-}$ mice reproduce several phenotypes associated with ASDs, a neurodevelopmental disorder (Schmeisser et al., 2012; Won et al., 2012; Ko et al., 2016). In this context, it is interesting that we have uncovered an unexpected neurodevelopmental phenotype in Shank2 $\Delta\text{ex}7^{-/-}$ mice: defective synapse maturation. A similar excess of silent synapses has been described in mice lacking Sapap3 (Wan et al., 2011), a GKAP family protein that directly interacts with SHANKs (Boeckers et al., 1999; Naisbitt et al., 1999; Yao et al., 1999). Of note, the loss of Sapap3 causes obsessive-compulsive behavioral traits in mice (Welch et al., 2007), which are typical in individuals with autism and have also been described in Shank2 $\Delta\text{ex}7^{-/-}$ mice (Schmeisser et al., 2012). Likewise, FMR1 $^{-/-}$ mice, a model for the autism-related fragile X syndrome, show altered plasticity and synapse maturation in the barrel cortex (Harlow et al., 2010). Last, in a mouse line with SYNGAP1 haploinsufficiency, a genetic model for intellectual disability and ASDs, hippocampal synapses are unsilenced prematurely, adversely impacting learning and memory in the adult animal (Rumbaugh et al., 2006; Clement et al., 2012). Together with the present findings, these studies draw a picture of synapse maturation as a tightly controlled process, the dysregulation of which seems of relevance for a range of neurodevelopmental disorders; the process of synaptic maturation should therefore be investigated further in future studies, in particular with regard to how it can be influenced by therapeutic approaches.

References

- Ballesteros JJ, Buschler A, Köhr G, Manahan-Vaughan D (2016) Afferent input selects NMDA receptor subtype to determine the persistency of hippocampal LTP in freely behaving mice. *Front Synaptic Neurosci* 8:33. [CrossRef](#)
- Berkel S, Marshall CR, Weiss B, Howe J, Roeth R, Moog U, Endris V, Roberts W, Szatmari P, Pinto D, Bonin M, Riess A, Engels H, Sprengel R, Scherer SW, Rappold GA (2010) Mutations in the SHANK2 synaptic scaffolding gene in autism spectrum disorder and mental retardation. *Nat Genet* 42:489–491. [CrossRef](#)
- Böckers TM, Segger-Junius M, Iglauer P, Bockmann J, Gundelfinger ED, Kreutz MR, Richter D, Kindler S, Kreienkamp H-J (2004) Differential expression and dendritic transcript localization of Shank family members: identification of a dendritic targeting element in the 3' untranslated region of Shank1 mRNA. *Mol Cell Neurosci* 26:182–190. [CrossRef](#)
- Boeckers TM, Winter C, Smalla KH, Kreutz MR, Bockmann J, Seidenbecher C, Garner CC, Gundelfinger ED (1999) Proline-rich synapse-associated proteins ProSAP1 and ProSAP2 interact with synaptic proteins of the SAPAP/GKAP family. *Biochem Biophys Res Commun* 264:247–252. [CrossRef](#)
- Boeckers TM, Liedtke T, Spilker C, Dresbach T, Bockmann J, Kreutz MR, Gundelfinger ED (2005) C-terminal synaptic targeting elements for postsynaptic density proteins ProSAP1/Shank2 and ProSAP2/Shank3. *J Neurochem* 92:519–524. [CrossRef](#)
- Bozdagi O, Sakurai T, Papapetrou D, Wang X, Dickstein DL, Takahashi N, Kajiwara Y, Yang M, Katz AM, Scattoni ML, Harris MJ, Saxena R, Silverman JL, Crawley JN, Zhou Q, Hof PR, Buxbaum JD (2010) Haploinsufficiency of the autism-associated Shank3 gene leads to deficits in synaptic function, social interaction, and social communication. *Mol Autism* 1:15. [CrossRef](#)
- Buschler A, Goh JJ, Manahan-Vaughan D (2012) Frequency dependency of NMDA receptor-dependent synaptic plasticity in the hippocampal CA1 region of freely behaving mice. *Hippocampus* 22:2238–2248. [CrossRef](#)
- Clement JPP, Aceti M, Creson TKK, Ozkan EDD, Shi Y, Reish NJJ, Almonte AGG, Miller BHH, Wiltgen BJJ, Miller CAA, Xu X, Rumbaugh G (2012) Pathogenic SYNGAP1 mutations impair cognitive development by disrupting maturation of dendritic spine synapses. *Cell* 151:709–723. [CrossRef](#)
- Du Y, Weed SA, Xiong WC, Marshall TD, Parsons JT (1998) Identification of a novel cortactin SH3 domain-binding protein and its localization to growth cones of cultured neurons. *Mol Cell Biol* 18:5838–5851. [CrossRef](#)
- Durand CM, Betancur C, Boeckers TM, Bockmann J, Chaste P, Fauchereau F, Nygren G, Rastam M, Carina I, Anckarsäter H, Sponheim E, Goubran-Botros H, Delorme R, Chabane N, De Mas P, Bieth E, Rogé B, Héron D, Burglen L, Gillberg C, et al. (2007) Mutations in the gene encoding the synaptic scaffolding protein SHANK3 are associated with autism spectrum disorders. *Nat Genet* 39:25–27. [CrossRef](#)
- Durand CM, Perroy J, Loll F, Perrais D, Fagni L, Bourgeron T, Montcouquiol M, Sans N (2012) SHANK3 mutations identified in autism lead to modification of dendritic spine morphology via an actin-dependent mechanism. *Mol Psychiatry* 17:71–84.
- Durand GM, Kovalchuk Y, Konnerth A (1996) Long-term potentiation and functional synapse induction in developing hippocampus. *Nature* 381:71–75. [CrossRef](#)
- Ebert DH, Greenberg ME (2013) Activity-dependent neuronal signaling and autism spectrum disorder. *Nature* 493:327–337. [CrossRef](#)
- Ehrlich I, Klein M, Rumpel S, Malinow R (2007) PSD-95 is required for activity-driven synapse stabilization. *Proc Natl Acad Sci U S A* 104:4176–4181. [CrossRef](#)
- Grabrucker AM, Knight MJ, Proepper C, Bockmann J, Joubert M, Rowan M, Nienhaus GU, Garner CC, Bowie JU, Kreutz MR, Gundelfinger ED, Boeckers TM (2011) Concerted action of zinc and ProSAP/Shank in synaptogenesis and synapse maturation. *EMBO J* 30:569–581. [CrossRef](#)
- Haeckel A, Ahuja R, Gundelfinger ED, Qualmann B, Kessels MM (2008) The actin-binding protein Abp1 controls dendritic spine morphology and is important for spine head and synapse formation. *J Neurosci* 28:10031–10044. [CrossRef](#)
- Harlow EG, Till SM, Russell TA, Wijetunge LS, Kind P, Contractor A (2010) Critical period plasticity is disrupted in the barrel cortex of FMR1 knockout mice. *Neuron* 65:385–398. [CrossRef](#)

- Harris KP, Akbergenova Y, Cho RW, Baas-Thomas MS, Littleton JT (2016) Shank Modulates Postsynaptic Wnt Signaling to Regulate Synaptic Development. *J Neurosci* 36:5820–5832. [Medline](#)
- Huang X, Stodieck SK, Goetze B, Cui L, Wong MH, Wenzel C, Hosang L, Dong Y, Löwel S, Schlüter OM (2015) Progressive maturation of silent synapses governs the duration of a critical period. *Proc Natl Acad Sci* 112:E3131–E3140. [CrossRef](#)
- Hung AY, Futai K, Sala C, Valtschanoff JG, Ryu J, Woodworth MA, Kidd FL, Sung CC, Miyakawa T, Bear MF, Weinberg RJ, Sheng M (2008) Smaller dendritic spines, weaker synaptic transmission, but enhanced spatial learning in mice lacking Shank1. *J Neurosci* 28:1697–1708. [CrossRef](#)
- Isaac JTR, Nicoll RA, Malenka RC (1995) Evidence for silent synapses: implications for the expression of LTP. *Neuron* 15:427–434. [CrossRef](#)
- Jiang Y, Ehlers MD (2013) Modeling autism by SHANK gene mutations in mice. *Neuron* 78:8–27. [CrossRef](#)
- Kim SM, Choi KY, Cho IH, Rhy JH, Kim SH, Park CS, Kim E, Song WK (2009) Regulation of dendritic spine morphology by SPIN90, a novel Shank binding partner. *J Neurochem* 109:1106–1117. [CrossRef](#)
- Kirov SA, Sorra KE, Harris KM (1999) Slices have more synapses than perfusion-fixed hippocampus from both young and mature rats. *J Neurosci* 19:2876–2886. [Medline](#)
- Ko H-G, Oh S-B, Zhuo M, Kaang B-K (2016) Reduced acute nociception and chronic pain in *Shank2*^{-/-} mice. *Mol Pain* 12:1744806916647056. [CrossRef](#)
- Kouser M, Speed HE, Dewey CM, Reimers JM, Widman AJ, Gupta N, Liu S, Jaramillo TC, Bangash M, Xiao B, Worley PF, Powell CM (2013) Loss of predominant Shank3 isoforms results in hippocampus-dependent impairments in behavior and synaptic transmission. *J Neurosci* 33:18448–18468. [CrossRef](#)
- Leblond CS, Heinrich J, Delorme R, Proepper C, Betancur C, Huguet G, Konyukh M, Chaste P, Ey E, Rastam M, Anckarsäter H, Nygren G, Gillberg IC, Melke J, Toro R, Regnault B, Fauchereau F, Mercati O, Lemièrre N, Skuse D, et al. (2012) Genetic and functional analyses of SHANK2 mutations suggest a multiple hit model of autism spectrum disorders. *PLoS Genet* 8:e1002521. [CrossRef](#)
- Lee E-J, Lee H, Huang T-N, Chung C, Shin W, Kim K, Koh J-Y, Hsueh Y-P, Kim E (2015) Trans-synaptic zinc mobilization improves social interaction in two mouse models of autism through NMDAR activation. *Nat Commun* 6:7168. [CrossRef](#)
- Liao D, Hessler NA, Malinow R (1995) Activation of postsynaptically silent synapses during pairing-induced LTP in CA1 region of hippocampal slice. *Nature* 375:400–404. [CrossRef](#)
- Lim CS, Kim H, Yu NK, Kang SJ, Kim TH, Ko HG, Lee J, Yang J, Ryu HH, Park T, Gim J, Nam HJ, Baek SH, Wegener S, Schmitz D, Boeckers TM, Lee MG, Kim E, Lee JH, Lee YS, et al. Kaang BK (2017) Enhancing inhibitory synaptic function reverses spatial memory deficits in Shank2 mutant mice. *Neuropharmacology* 112:104–112. [CrossRef](#)
- Lim S, Naisbitt S, Yoon J, Hwang JI, Suh PG, Sheng M, Eunjoon K (1999) Characterization of the Shank family of synaptic proteins. Multiple genes, alternative splicing, and differential expression in brain and development. *J Biol Chem* 274:29510–29518. [CrossRef](#)
- Lim S, Sala C, Yoon J, Park S, Kuroda S, Sheng M, Kim E (2001) Sharpin, a novel postsynaptic density protein that directly interacts with the shank family of proteins. *Mol Cell Neurosci* 17:385–397. [CrossRef](#)
- MacGillavry HD, Kerr JM, Kassner J, Frost NA, Blanpied TA (2016) Shank-cortactin interactions control actin dynamics to maintain flexibility of neuronal spines and synapses. *Eur J Neurosci* 43:179–193. [CrossRef](#)
- Marie H, Morishita W, Yu X, Calakos N, Malenka RC (2005) Generation of silent synapses by acute in vivo expression of CaMKIV and CREB. *Neuron* 45:741–752. [CrossRef](#)
- Naisbitt S, Kim E, Tu JC, Xiao B, Sala C, Valtschanoff J, Weinberg RJ, Worley PF, Sheng M (1999) Shank, a novel family of postsynaptic density proteins that binds to the NMDA receptor/PSD-95/GKAP complex and cortactin. *Neuron* 23:569–582. [CrossRef](#)
- Nicoll RA (2017) A brief history of long-term potentiation. *Neuron* 93:281–290. [CrossRef](#)
- Peça J, Feliciano C, Ting JT, Wang W, Wells MF, Venkatraman TN, Lascola CD, Fu Z, Feng G (2011) Shank3 mutant mice display autistic-like behaviours and striatal dysfunction. *Nature* 472:437–442. [CrossRef](#)
- Peter S, ten Brinke MM, Stedehouder J, Reinelt CM, Wu B, Zhou H, Zhou K, Boele H-J, Kushner SA, Lee MG, Schmeisser MJ, Boeckers TM, Schonewille M, Hoebeek FE, De Zeeuw CI (2016) Dysfunctional cerebellar Purkinje cells contribute to autism-like behaviour in Shank2-deficient mice. *Nat Commun* 7:12627. [CrossRef](#)
- Roussignol G, Ango F, Romorini S, Tu JC, Sala C, Worley PF, Bockaert J, Fagni L (2005) Shank expression is sufficient to induce functional dendritic spine synapses in aspiny neurons. *J Neurosci* 25:3560–3570. [CrossRef](#)
- Rumbaugh G, Adams JP, Kim JH, Haganir RL (2006) SynGAP regulates synaptic strength and mitogen-activated protein kinases in cultured neurons. *Proc Natl Acad Sci U S A* 103:4344–4351. [CrossRef](#)
- Sala C, Pièch V, Wilson NR, Passafaro M, Liu G, Sheng M (2001) Regulation of dendritic spine morphology and synaptic function by Shank and Homer. *Neuron* 31:115–130. [CrossRef](#)
- Sato D, Lionel AC, Leblond CS, Prasad A, Pinto D, Walker S, O'Connor I, Russell C, Drmic IE, Hamdan FF, Michaud JL, Endris V, Roeth R, Delorme R, Huguet G, Leboyer M, Rastam M, Gillberg C, Lathrop M, Stavropoulos DJ, et al. (2012) SHANK1 deletions in males with autism spectrum disorder. *Am J Hum Genet* 90:879–887. [CrossRef](#)
- Schmeisser MJ, Ey E, Wegener S, Bockmann J, Stempel AV, Kuebler A, Janssen A-L, Udvardi PT, Shiban E, Spilker C, Balschun D, Skryabin BV, Dieck S, tom Smalla K-H, Montag D, Leblond CS, Faure P, Torquet N, Le Sourd A-M, Toro R, et al. (2012) Autistic-like behaviours and hyperactivity in mice lacking ProSAP1/Shank2. *Nature* 486:256–260. [CrossRef](#)
- Sheng M, Kim E (2000) The Shank family of scaffold proteins. *J Cell Sci* 113:1851–1856.
- Shi R, Redman P, Ghose D, Liu Y, Ren X, Ding LJ, Liu M, Jones KJ, Xu W (2017) Shank proteins differentially regulate synaptic transmission. *eNeuro* 4:ENEURO.0163-15.2017. [CrossRef](#)
- Stanika RI, Flucher BE, Obermair GJ (2015) Regulation of postsynaptic stability by the L-type calcium channel CaV1.3 and its interaction with PDZ proteins. *Curr Mol Pharmacol* 8:95–101. [CrossRef](#)
- Verpelli C, Dvoretzskova E, Vicidomini C, Rossi F, Chiappalone M, Schoen M, Di Stefano B, Mantegazza R, Broccoli V, Böckers TM, Dityatev A, Sala C (2011) Importance of Shank3 protein in regulating metabotropic glutamate receptor 5 (mGluR5) expression and signaling at synapses. *J Biol Chem* 286:34839–34850. [CrossRef](#)
- Wan Y, Feng G, Calakos N (2011) Sapap3 Deletion Causes mGluR5-Dependent Silencing of AMPAR Synapses. *J Neurosci* 31:16685–16691. [CrossRef](#)
- Wang X, McCoy PA, Rodriguiz RM, Pan Y, Je HS, Roberts AC, Kim CJ, Berrios J, Colvin JS, Bousquet-Moore D, Lorenzo I, Wu G, Weinberg RJ, Ehlers MD, Philpot BD, Beaudet AL, Wetsel WC, Jiang Y-H (2011) Synaptic dysfunction and abnormal behaviors in mice lacking major isoforms of Shank3. *Hum Mol Genet* 20:3093–3108. [CrossRef](#)
- Welch JM, Lu J, Rodriguiz RM, Trotta NC, Peca J, Ding J-D, Feliciano C, Chen M, Adams JP, Luo J, Dudek SM, Weinberg RJ, Calakos N, Wetsel WC, Feng G (2007) Cortico-striatal synaptic defects and OCD-like behaviours in Sapap3-mutant mice. *Nature* 448:894–900. [CrossRef](#)
- Won H, Lee H-R, Gee HY, Mah W, Kim J-I, Lee J, Ha S, Chung C, Jung ES, Cho YS, Park S-G, Lee J-S, Lee K, Kim D, Bae YC, Kaang B-K, Lee MG, Kim E (2012) Autistic-like social behaviour in Shank2-mutant mice improved by restoring NMDA receptor function. *Nature* 486:261–265. [CrossRef](#)
- Yao I, Hata Y, Hirao K, Deguchi M, Ide N, Takeuchi M, Takai Y (1999) Synamon, a novel neuronal protein interacting with synapse-associated protein 90/postsynaptic density-95-associated protein. *J Biol Chem* 274:27463–27466. [CrossRef](#)